Polyhedral silver clusters as single molecule ammonia sensor based on charge transfer-induced plasmon enhancement

Jiu-Huan Chen(陈九环)[1] and Xin-Lu Cheng(程新路)[1,2,†]

[1] *Institute of Atomic and Molecular Physics, Sichuan University, Chengdu* 610065, *China*
[2] *Key Laboratory of High Energy Density Physics and Technology of Ministry of Education, Sichuan University, Chengdu* 610065, *China*

(Received 6 March 2022; revised manuscript received 27 April 2022; accepted manuscript online 7 May 2022)

The unique plasmon resonance characteristics of nanostructures based on metal clusters have always been the focus of various plasmon devices and different applications. In this work, the plasmon resonance phenomena of polyhedral silver clusters under the adsorption of NH_3, N_2, H_2, and CH_4 molecules are studied by using time-dependent density functional theory. Under the adsorption of NH_3, the tunneling current of silver clusters changes significantly due to the charge transfer from NH_3 to silver clusters. However, the effects of N_2, H_2, and CH_4 adsorption on the tunneling current of silver clusters are negligible. Our results indicate that these silver clusters exhibit excellent selectivities and sensitivities for NH_3 detection. These findings confirm that the silver cluster is a promising NH_3 sensor and provide a new method for designing high-performance sensors in the future.

Keywords: ammonia, Ag clusters, plasmon, tunneling current spectrum

PACS: 73.20.Mf, 71.45.Gm, 78.67.Bf **DOI:** 10.1088/1674-1056/ac6daf

1. Introduction

In view of its potential harm to the surrounding environment and public health, ammonia has been one of the objects detected by gas sensor. Metal oxides have been extensively studied as gas sensors based on the resistance changes caused by the adsorption of gas molecules.[1,2] Transition-metal dichalcogenides exhibit excellent performance in gas sensor applications due to their lower band gaps and better conductivities.[3] Owing to high mobility, excellent mechanical properties and high surface area, two-dimensional materials (black phosphoene, stanane, carbon nitride, *etc*.) have gradually become the candidate materials of sensors.[4–6] In addition, some investigations show the potential applications of nanotube materials in high-performance ammonia gas sensors.[7] The performance of the sensor is effectively improved through strategies such as doping, hydrogenation, and fluorination, which greatly expands the application range of the sensor.[8–10] In recent years, gas sensors based on nanoclusters have been favored by researchers due to their better sensitivities and selectivities.[11,12]

Metal nanoparticles have attracted widespread attention in the fields of science and technology due to their unique optical, electronic and catalytic properties. The localized surface plasmon resonance[13–15] maintained by the nanostructure due to its limited boundary will bring about localized optical waveguides, charge accumulation, and localized field enhancement near the surface.[16] Many novel effects caused by surface plasmon excitation, such as local field strength enhancement effect,[17] negative refraction phenomena,[18] and Fano-like chiroptical response,[19] have been applied to biosensing,[20] photocatalysis,[21] cancer treatment,[22] *etc*. In recent years, owing to the enhancement of the electric field strength at the sharp corners and edges, plasmonic nanoparticles with various polyhedral shapes have become a research hotspot.[23] With the rapid improvement of the process technology, silver cluster structures with different shapes have been successfully synthesized in laboratory. Based on the PVP synthesis process, the specific polyhedral shapes have been successfully manufactured.[24] So far, thermal and electrochemical methods have also been used to exclusively synthesize gold and silver nanoprisms. Millstone *et al*. reported a synthetic procedure to produce relatively homogeneous triangular gold nanoparticles which have an average edge length of nanometer.[25] Yu *et al*. theoretically studied the optical absorption spectra for spherical Ag_n clusters ($n = 5$–120) embedded in solid Ne.[26] These research results show that the plasmonic characteristic reveals striking distinction and dependence on the structure shape and size. There has not been any research on the properties of other polyhedral silver clusters at the nanometer size.

Research results have shown that the presence of molecules that cause the local refractive index to change has a better tuning effect on the spectrum of surface plasmon resonance.[27] It is proved that the material exhibits many fantastic nonlinear phenomena under the influence of laser field.[28] Yan *et al*.[29] studied the nonlinear response of a linear silver atomic chain upon ultrafast laser excitation in real

†Corresponding author. E-mail: chengxl@scu.edu.cn

© 2023 Chinese Physical Society and IOP Publishing Ltd

time by using the time-dependent density functional theory. What is surprising is that up to the fifth-order nonlinear response occurs in the current spectrum. Shinde and Singh analyzed the effect of the application of ultrafast and femtosecond laser to the nonlinear electron dynamics in phosphorene.[30] Recently, Zhang *et al*. investigated the ultrafast carrier dynamics of plasmon-mediated photoreduction of CO_2 and NH_3 photodecomposition on silver nanoclusters at a single molecular level.[31,32] These findings provide in-depth insights into designing plasmon-mediated photocatalysts with high efficiency. However, the research of silver cluster nanostructures in NH_3 sensor is still lacking.

Here, we conduct the simulation study of the plasmonic performance of several polyhedral Ag clusters under the action of femtosecond laser. The effects of NH_3, N_2, CH_4, and H_2 adsorption on the optical properties of silver clusters are investigated. Time-dependent density functional theory proves to be an effective method. The tunneling current spectrum of silver clusters change significantly upon interaction with NH_3 molecules. However, the plasmon resonance behaviors of silver clusters are not sensitive to the N_2 nor H_2 nor CH_4 adsorption. These findings demonstrate that silver cluster nanostructures have superior application prospects in ammonia gas detection sensors.

2. Computational methods

Our simulation calculations were carried out by using OCTOPUS software based on time-dependent density functional theory.[33] In the calculation process of ground state and excited state, the method of local-density approximation (LDA) was applied to the exchange correlation potential.[34] These atoms in these systems were determined by Troullier–Martins pseudopotential.[35] The radius of the sphere centered on each atom was 6 Å and simulation area was divided by a uniform grid of 0.3 Å. The spectra of absorption and tunneling current were obtained by propagating Kohn–Sham wave functions for some time. We considered the optical properties under impulse excitation $E(t) = E_0\delta(t)$ and Gaussian wavepackets of laser pulses. For the time evolution, we used the total time of $90\hbar/\text{eV} \approx 60$ fs in time steps of $0.003\hbar/\text{eV} \approx 0.002$ fs.

In this study, we chose the polyhedral Ag_7 (decanedron), Ag_8 (dodecahedron), Ag_{19} (triacontahedron) nanoclusters as the research objects. The optimized structural parameters are consistent with the results reported in previous literature.[36–38] The geometry of these Ag clusters is almost unchanged upon adsorption. In the optimization process for Ag_n–gas, we fixed the silver atom. This treatment hardly affected the plasmon resonance frequency of these systems. These optimized structures of these research systems are shown in Fig. 1.

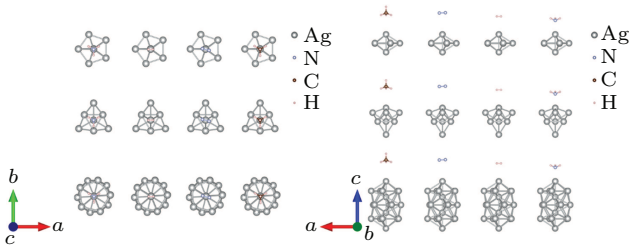


Fig. 1. Schematic diagram of Ag_n ($n = 7$, 8, 19) and Ag_n–gas nanostructures.

3. Results and discussion

In order to explore the possibility of the silver clusters as gas sensors for NH_3 detection, we first examine the optical absorption spectra for Ag clusters with different shapes and the effect of NH_3 molecular adsorption, and the results are shown in Fig. 2. The polarization direction of the incident laser pulse is selected to be parallel to the Z axis direction. Sharp contrasts are observed in the spectral behavior of these systems. We find that the absorption spectra of these nanostructures reveal many sharp peaks, which is attributed to the obvious dispersion of electronic energy levels caused by the quantum confinement effect.[26,39] As the size of the structure increases, the plasmon resonance also exhibits a red shift. This arises from the continuous decrease of the energy level spacing of the silver clusters caused by the superposition of single electron orbitals.[40] Meanwhile, the strength of the most significant absorption peak is enhanced with size increasing. This phenomenon reveals that more electrons participate in collective oscillation. This phenomenon is consistent with those of other materials, such as noble metal nanospheroids and aluminum nanoparticle.[41,42] In the case of NH_3 adsorption, there is a distinct shift of absorption peak. It is also interesting to note that there are some smaller resonance peaks for Ag_n–NH_3. This stems from the hybridization of NH_3 molecular orbitals and Ag atomic orbitals and the number of orbitals increasing with the number of atoms.

To explore the feasibility of NH_3 molecular detection of Ag_7 cluster, we investigate the effect of adsorption of molecular gases (NH_3, N_2, H_2, CH_4) on the tunneling current response under the action of laser with the frequency 2.41 eV. We present the optical response of these systems to ultrafast femtosecond laser pulses, which are expressed by the equation of the time variation of optical field $E(t)$ as

$$E(t) = E_0 \exp\left[-(t-t_0)^2/2\tau^2\right] \cos(\omega t - \omega t_0). \tag{1}$$

The maximum intensity of laser field is $E_0 = 0.01\ \text{V}\cdot\text{Å}^{-1}$, and we set the width $\tau = 3.3$ fs, and $t_0 = 10$ fs. The frequency, ω, is determined, which is dependent on the photoabsorption energy peak of research objects. The evolution of the laser over time is shown in Fig. 3.

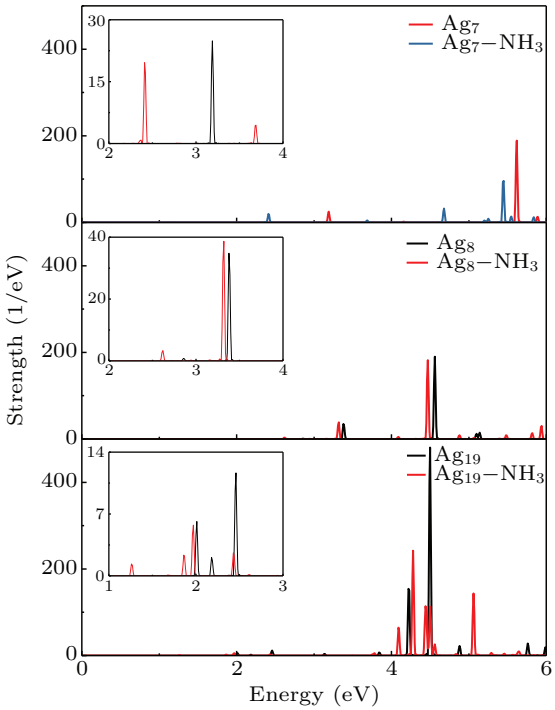


Fig. 2. Absorption spectra of Ag_n and Ag_n–NH_3 nanostructures with polarization direction parallel to Z axis.

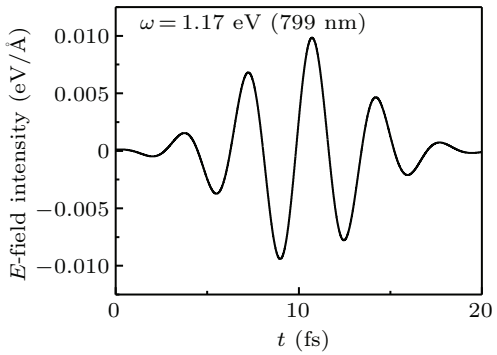


Fig. 3. Laser oscillograph with maximum laser intensity $E_{max} = 0.01$ V/Å.

The current plane is located in the central plane between Ag_7 cluster and gas molecule. For the Ag_7 structure, the current plane is at the same position. The current density is given by

$$j(z,t) = -\frac{\mathrm{i}\hbar}{2}\sum_k \{\varphi_k^* \nabla\varphi_k(z,t) - \varphi_k(z,t)\nabla\varphi_k^*(z,t)\}. \quad (2)$$

The current can be obtained by integrating over the specified plane S which is parallel to the XZ plane, specifically is expressed as

$$I(t) = \int_S j(z,t)\cdot \mathrm{d}S. \quad (3)$$

The current spectrum in the frequency domain can be obtained by taking the Fourier transform as follows:

$$I(\omega) = \int I(t)\,\mathrm{e}^{\mathrm{i}\omega t}\,\mathrm{d}t. \quad (4)$$

The time evolution of tunneling currents of Ag_7 cluster in the presence of different molecules are shown in Fig. 4(a). For comparison, the tunneling current of isolated Ag_7 cluster is also given. In addition, the obtained current as a function of excitation energy is displayed in Fig. 4(b). For different molecular adsorption situations, the tunneling current exhibits distinct oscillation modes. For Ag_7–H_2 and Ag_7–CH_4, the tunneling currents seem to vanish with the attenuation of the laser field. But for other systems, the tunneling currents exhibit coherent oscillation in the duration of the laser pulse. After the external field decays, the tunneling current appears as a continuous oscillation for each of different waveforms. For the NH_3 adsorption, the strength of tunneling current is the largest, reaching 0.002 mA. This is consistent with the strong absorption intensity at this frequency in Fig. 4(b). These phenomena are consistent with the previously reported nonlinear resonance of plasmonic system that can be distinctly tuned by coupling with molecules. This phenomenon is attributed to the influence of the adsorption environment on the plasmon resonance of the material. According to the above analysis, we can predict that the Ag_7 cluster may be a very effective sensor for detecting NH_3 from N_2, H_2, and CH_4 by measuring the signal of the tunneling current responsing to gas adsorption.

In order to explore the physical mechanism of oscillation modes at different frequencies, we analyze the Fourier transform distribution of induced charges at the resonance frequency. The charge density distribution appears as a quadrupole mode for the isolated Ag_7 cluster as shown in Fig. 4(c). However, the density response presents a second order charge transfer pattern of dipolar plasmonic excitation for NH_3 molecule adsorbed on the Ag_7 cluster (Fig. 4(d)). This is considered to be an excitation behavior of a multiple-order oscillation mode. This phenomenon is consistent with the plasmon excitation mode in the silver atom chain.[29] For the Ag_7–N_2 system, the induced charge density shows the dipolar characteristics along the excitation direction of the laser pulse (Fig. 4(e)). It is also worth noting that the induced charge concentration in Ag_7–NH_3 is an order of magnitude higher than that in other systems, which explains the relatively strong resonance peak of the tunneling current. These results indicate that different plasmonic modes are excited in these systems under the action of laser pulse.

The tunneling current response of the Ag_8 and Ag_{19} cluster can be conveniently manipulated by adsorption environment. It is obvious that the current response signals show significant distinctions under laser excitation for silver clusters with different configurations. For these two clusters, we use the laser excitation with frequencies of 3.06 eV and 1.17 eV, respectively. As shown in Fig. S1, it shows the time evolution of the tunnel currents for Ag_8 cluster without and with gas molecule. For the Ag_8 cluster, the tunneling current intensity of the silver cluster system increases twice when NH_3 is adsorbed. The tunneling current intensity of the silver clus-

ters hardly change, in view of the consideration of N_2, H_2, and CH_4 adsorption. From the spatial distribution of the induced charge response at the resonance frequency, it follows that the distribution of induced charges is not affected by N_2 nor H_2 nor CH_4 (Fig. S2). It is worth noting that the charge concentration involved in plasmon resonance increases in the Ag_8–NH_3 system, which is consistent with the stronger absorption peak appearing in the tunneling current spectrum (Fig. S3). For the Ag_{19} cluster, our results show superior selectivity toward the NH_3 molecule. However, the tunneling current signal is relatively weak (Figs. S4 and S5). To enhance the intensity of the detection signal, we consider the effect of the laser intensity on the cluster tunneling current response. The results show that the tunneling current signal of Ag–NH_3 complex can be enhanced by using a stronger laser (Figs. S6 and S7). In addition, we investigate the larger size Ag clusters, and the results show that Ag_{25} cluster still presents the excellent performance in NH_3 sensing with the increase of structure size (Fig. S8).

The effect of NH_3 adsorption on the optical response of Ag clusters is attributed to the charge transfer. To confirm this argument, figure 5 shows the tunneling current resonance as a function of electron doping. Adding net electrons, the Ag clusters exhibit a tunneling current induced by the laser pulse. Moreover, the oscillation mode and strength of the tunneling current is strongly associated with the quantity of charge. We can see that the induced charge density distribution is significantly distinct at different resonance frequencies. The regulation of plasmon performance by adding or removing electrons has been observed in one-dimensional (BN)n/Cm/(BN)n quantum-well structures.[43] In order to better explain the mechanism of the tunneling current resonance phenomenon, we further investigate the localization distribution characteristics of electrons as shown in Fig. 6. For these different complexes, only in the case of adsorption of NH_3 molecules can the charges transfer from cluster to adsorbed molecules. This is consistent with what we observed and also confirm the argument for induced charge transfer.

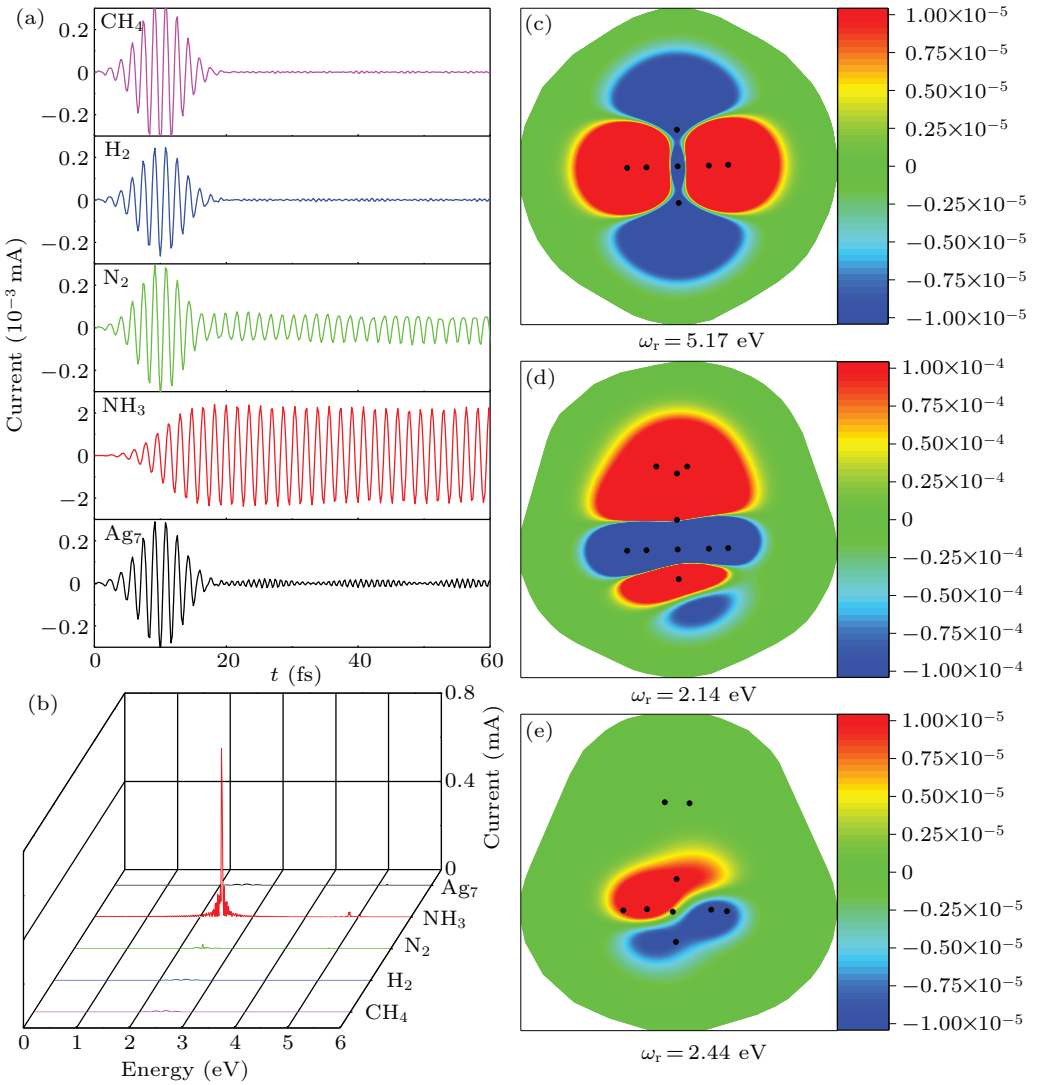


Fig. 4. (a) Time evolution of tunnel currents for Ag_7 cluster without and with gas molecule, with incident laser pulse frequency being 2.41 eV. (b) Corresponding tunneling current spectra for Ag_7 cluster without and with gas molecule. (c)–(e) Fourier transform of time-evolved charge densities projected in the YZ plane at different peak frequencies for the Ag_7, Ag_7–NH_3, and Ag_7–N_2, with ω_r denoting frequency of the resonance peak.

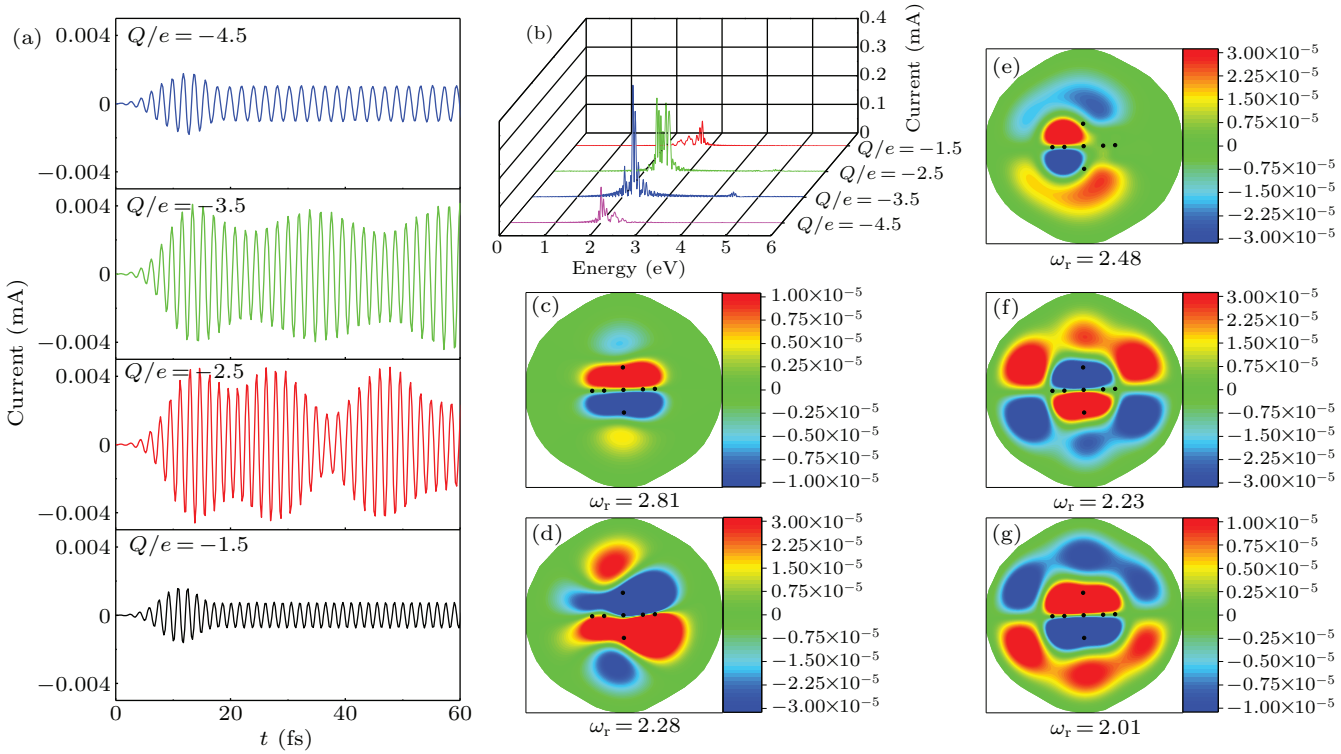


Fig. 5. (a) Time evolution of tunnel currents for Ag_7 cluster with different net charges, where incident laser pulse frequency is 2.41 eV. (b) Tunneling current spectrum of Ag_7 cluster as a function of net doped charge Q/e. (c)–(g) Induced charge density distributions of Ag_7 cluster with different net charges at resonance energy point.

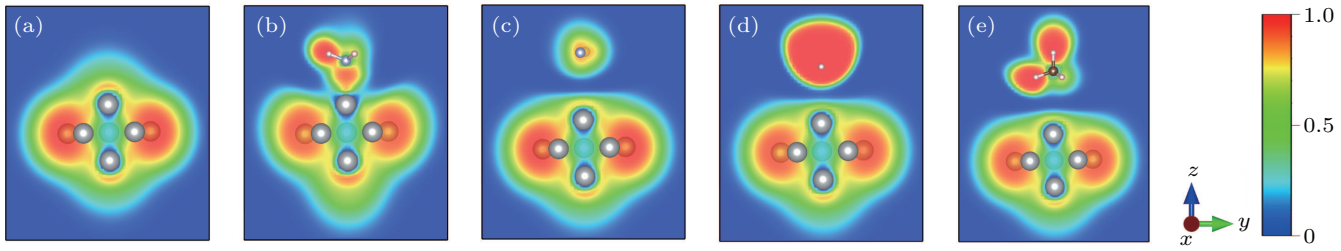


Fig. 6. Electron localization function (ELF) of silver clusters without and with different gas molecule: (a) ELF of Ag_7 cluster, (b)–(e) ELF of Ag_7 cluster with NH_3, N_2, H_2, and CH_4, respectively.

4. Conclusions

According to the time-dependent density functional theory, we have studied the plasmonic properties of NH_3, N_2, H_2, and CH_4 molecules on the polyhedral Ag clusters. The plasmon resonance frequency depends on the shape of cluster, which is the reason for selecting different excitation frequency of the laser pulse. The adsorption of NH_3 molecule triggers off remarkable change in tunneling current spectrum of Ag_n clusters. We demonstrate that the regulation of plasmon performance by NH_3 adsorption is attributable to the charge transfer between NH_3 molecules and clusters. To date, atomically precise metal cluster structures with various shapes have also been successfully synthesized experimentally.[44,45] Therefore, it is feasible to fabricate silver cluster nanosensors. Overall, the present work proves that these clusters' structures can be used as a promising gas sensor for NH_3 detection.

Acknowledgements

Project supported by the National Natural Science Foundation of China (Grant Nos. 11774248 and 11974253) and the National Key Research and Development Program of China (Grant No. 2017YFA0303600).

References

[1] Wei W, Li W and Wang L 2018 *Sensors and Actuators B: Chemical* **263** 502
[2] Li P, Wang B, Qin C, Han C, Sun L and Wang Y 2020 *Ceramics International* **46** 19232
[3] Järvinen T, Lorite G S, Peräntie J, Toth G, Saarakkala S, Virtanen V K and Kordas K 2019 *Nanotechnology* **30** 405501
[4] Faye O, Eduok U and Szpunar J A 2019 *J. Phys. Chem. C* **123** 29513
[5] Yong Y, Cui H, Zhou Q, Su X, Kuang Y and Li X 2019 *Appl. Surf. Sci.* **487** 488
[6] Kumar V and Roy D R 2019 *Physica E* **110** 100
[7] Li R, Jiang K, Chen S, Lou Z, Huang T, Chen D and Shen G 2017 *RSC Adv.* **7** 52503
[8] Ali I, Kashyout A E-H B, Tayel M, Shokry Hassan H and Rizk M 2020 *J. of Mater. Res. Technol.* **9** 15693

[9] Yong Y, Zhou Q, Su X, Kuang Y, Catlow C R A and Li X 2019 *Journal of Molecular Liquids* **289** 111153
[10] Liu Y, Shi T T, Chen T, He W J, Chen M M and Cao D 2019 *Sensors and Actuators B: Chemical* **281** 789
[11] Yong Y, Li C, Li X, Li T, Cui H and Lv S 2015 *J. Phys. Chem. C* **119** 7534
[12] Yong Y, Li X, Zhou Q, Su X, Li T, Cui H and Lv S 2016 *RSC Adv.* **6** 26809
[13] Chen H, Chen Z, Yang H, Wen L, Yi Z, Zhou Z, Dai B, Zhang J, Wu X and Wu P 2022 *RSC Adv.* **12** 7821
[14] Zhao F, Lin J, Lei Z, Yi Z, Qin F, Zhang J, Liu L, Wu X, Yang W and Wu P 2022 *Phys. Chem. Chem. Phys.* **24** 4871
[15] Jiang L, Yi Y, Tang Y, Li Z, Yi Z, Liu L, Chen X, Jian R, Wu P and Yan P 2022 *Chin. Phys. B* **31** 038101
[16] Huang Y, Fang Y, Zhang Z, Zhu L and Sun M 2014 *Light: Science & Applications* **3** e199
[17] Brolo A G, Gordon R, Leathem B and Kavanagh K L 2004 *Langmuir* **20** 4813
[18] Huang H, Wang B, Long H, Wang K and Lu P 2014 *Opt. Lett.* **39** 5957
[19] Tian X, Sun S, Leong E S P, Zhu G, Teng J, Zhang B, Fang Y, Ni W and Zhang C Y 2020 *Phys. Chem. Chem. Phys.* **22** 3604
[20] Lim W Q and Gao Z 2016 *Nano Today* **11** 168
[21] Zhang Z, Zhang C, Zheng H and Xu H 2019 *Acc. Chem. Res.* **52** 2506
[22] Farokhnezhad M and Esmaeilzadeh M 2019 *Phys. Chem. Chem. Phys.* **21** 18352
[23] Shahriar Sabuktagin M and Syifa Hamdan K 2020 *Royal Society Open Science* **7** 191926
[24] Tao A, Sinsermsuksakul P and Yang P 2006 *Angew. Chem. Int. Ed.* **45** 4597
[25] Millstone J E, Park S, Shuford K L, Qin L, Schatz G C and Mirkin C A 2005 *J. Am. Chem. Soc.* **127** 5312
[26] Yu C, Schira R, Brune H, von Issendorff B, Rabilloud F and Harbich W 2018 *Nanoscale* **10** 20821
[27] Kazuma E, Jung J, Ueba H, Trenary M and Kim Y 2018 *Science* **360** 521
[28] Li M T, Liu M and Sun H B 2019 *Phys. Chem. Chem. Phys.* **21** 24262
[29] Yan L, Guan M and Meng S 2018 *Nanoscale* **10** 8600
[30] Shinde R and Singh A K 2018 *J. Phys. Chem. C* **122** 19146
[31] Zhang Y, Meng W, Chen D, Zhang L, Li S and Meng S 2022 *Nano Research* **15** 3894
[32] Zhang Y, Chen D, Meng W, Xu Z, Guo H, Li S and Meng S 2021 *J. Phys. Chem. C* **125** 26348
[33] Castro A, Appel H, Oliveira M, Rozzi C A, Andrade X, Lorenzen F, Marques M A L, Gross E K U and Rubio A 2006 *Phys. Status Solidi (b)* **243** 2465
[34] Ceperley D and Alder B 1980 *Phys. Rev. Lett.* **45** 567
[35] Troullier N and Martins J L 1991 *Phys. Rev. B* **43** 1993
[36] Xiong R, Die D, Xu Y G, Zheng B X and Fu Y C 2018 *Phys. Chem. Chem. Phys.* **20** 15824
[37] McKee M L and Samokhvalov A 2017 *J. Phys. Chem. A* **121** 5018
[38] Jiang Y Q, Peng P, Wen D D, Han S C and Hou Z Y 2015 *Comput. Mater. Sci.* **99** 156
[39] Jin R 2010 *Nanoscale* **2** 343
[40] Haifeng Y and Chunhua Z 2014 *Chin. J. Comput. Phys.* **31** 713
[41] Kooij E S, Ahmed W, Zandvliet H J W and Poelsema B 2011 *J. Phys. Chem. C* **115** 10321
[42] Mokkath J H and Henzie J 2020 *Phys. Chem. Chem. Phys.* **22** 1416
[43] Zhang K, Zhang H and Cheng X 2016 *Chin. Phys. B* **25** 037104
[44] Jin R, Zeng C, Zhou M and Chen Y 2016 *Chem. Rev.* **116** 10346
[45] Qin Z, Zhang J, Wan C, Liu S, Abroshan H, Jin R and Li G 2020 *Nat. Commun.* **11** 6019